Nucleus-nucleus collisions and interpretation of cosmic-ray cascades

J. Engel and T. K. Gaisser
Bartol Research Institute, University of Delaware, Newark, Delaware 19716

Paolo Lipari
Dipartimento di Fisica, Universitá di Roma, Piazzale Aldo Moro 2, Rome, Italy

Todor Stanev
Bartol Research Institute, University of Delaware, Newark, Delaware 19716
(Received 14 May 1992)

We describe a multiple scattering model of nucleus-nucleus collisions for use in simulation of atmospheric cascades produced by high-energy cosmic-ray nuclei. We emphasize the importance of a realistic treatment of nuclear fragmentation of the incident nucleus for fluctuations in quantities such as high-energy muon bundles and longitudinal development of giant air showers. The model is realized in a cascade program that can be combined with any treatment of hadronic interactions.

PACS number(s): 96.40.Pq, 24.10.Ht, 25.75.+r, 96.40.Tv

I. INTRODUCTION

At energies above 100 TeV, it becomes impractical to study the composition of the primary cosmic radiation directly because the flux is too low. Instead, one must study properties of the air showers induced by primary nuclei. A first approximation in this process employs the so-called "superposition model," in which a shower produced by a nucleus of mass A is equivalent to the superposition of A nucleon showers. In this model the effect of the incident nucleus is completely specified by the distribution of the positions of first interaction of the nucleons that compose the nucleus. Superposition implies an exponential distribution characterized by the nucleon interaction length.

In reality, when a nucleus enters the atmosphere it quickly interacts, because the interaction length for a heavy nucleus is very small. However, usually only one or a few of its nucleons scatter inelastically at this first point. Several spectator nucleons, light fragments, and usually one heavy fragment are also released in the interaction. These must be followed through subsequent collisions until all nucleons from the initial nucleus have interacted inelastically.

A natural extension of the superposition model, which we will call the "semisuperposition" model, retains the idea that a nucleus-induced shower is the superposition of A nucleon showers, but uses a "realistic" distribution of the positions of their first interaction. The new distribution of nucleon-subshower starting points reflects the properties of nucleus-air cross sections and of the fragmentation of the residual nuclei composed of spectator nucleons.

In this paper we develop the semisuperposition model in detail. It is still only approximate because it neglects the correlations between the number of interacting nucleons and the properties of the resulting inelastic interactions. We have two reasons for describing the results of this intermediate model. The first is that many existing cascade calculations are set up to treat nuclear showers as a set of A independent-nucleon-induced showers with a specified set of starting points. The second is that this simplified model is sufficient to encompass the important enhancement of fluctuations in showers associated with a realistic treatment of nuclear disintegration in the atmosphere.

To develop the semisuperposition model, we need three fundamental elements: (i) the nucleus-nucleus cross sections, (ii) the probability that in an inelastic nucleus-nucleus collision a number n of the projectile nucleons "participate," and (iii) the fragmentation probabilities of residual nuclei.

This work is organized as follows. In the next section we review the standard Glauber formalism [1] for nucleus-nucleus scattering [2]. We show how the "production" cross section can be expanded as a sum of partial cross sections for given numbers of "wounded" nucleons in the target or in the projectile nucleus. In Sec. III we treat the fragmentation of the residual nucleus, combining an estimate of deposited energy with the statistical decay model [3].

In Sec. IV we discuss the realistic distribution of the points of first interaction in showers induced by a primary nucleus. We obtain a simple and useful result which determines the average values of all observable shower parameters: For any additive measurable quantity Q, the semisuperposition model predicts the same average properties as the superposition model $\langle Q \rangle_A = A \langle Q \rangle_p$, i.e., A times the average value for the quantity computed in a proton shower of energy $E_p = E_A / A$. However, the fluctuations are significantly wider than in the superposition model. The wider fluctuations reflect correlations among nucleons in the same nucleus.

In Sec. V we present two examples directly related to experiment: the production of TeV muons by primary

nuclei with energy $E_A \sim 10^{15}$ eV and the development of shower size as a function of depth for primary nuclei of energy $E_A \sim 10^{18}$ eV. For these illustrative examples, we deliberately use a very simple interaction model to calculate production of secondary particles in interactions of wounded nucleons. The nuclear fragmentation algorithm can be used with any interaction model for nucleon-nucleon collisions, and the fluctuation effects (relative to superposition) are expected to be largely independent of the hadronic interaction model.

In Sec. VI we briefly discuss the limitations of the semisuperposition model and the modifications that can be expected from additional nuclear effects that are omitted in the semisuperposition picture. This section also includes some information about our underlying model of high-energy hadronic interactions [4], which is closely related to the dual parton model [5] with minijets as embodied in FRITJOF [6], PYTHIA [7], and HIJING [8]. The principal difference of our approach is that we focus on fragmentation properties of interactions at all impact parameters.

In Appendix A we list the formulas we have used for nuclear density profiles. Appendix B describes the approximations we make within standard Glauber theory. Appendix C includes some details of fluctuations in the semisuperposition model.

All the algorithms discussed here exist as a set of FORTRAN programs that are available on request.

II. NUCLEUS-NUCLEUS CROSS SECTIONS

We will consider the interaction of a projectile nucleus of mass A with a target nucleus of mass B. We denote the probability of an inelastic collision between nucleon j of nucleus A and nucleon k of nucleus B by P_{jk}. This probability is a function of the relative impact parameter of the two nucleons and can be expressed in terms of the nucleon-nucleon profile function Γ as

$$P_{jk} = P(|\mathbf{s}_j - \mathbf{t}_k + \mathbf{b}|) = 1 - |1 - \Gamma(|\mathbf{s}_j - \mathbf{t}_k + \mathbf{b}|)|^2 , \quad (1)$$

where $\mathbf{s}_j = \mathbf{r}_{\perp j}^{(B)}$ and $\mathbf{t}_k = \mathbf{r}_{\perp k}^{(A)}$ are transverse distances from the centers of A and B, respectively, and b is the impact parameter of the two nuclei relative to each other. The definition of Γ and the derivation of Eq. (1) appear in Appendix B.

The production cross section for the interaction between two nuclei of mass A and B can then be written as

$$\sigma_{AB} = \int d^2b \int [dr_A] \int [dr_B] \left\{ 1 - \prod_{k=1}^{A} \prod_{j=1}^{B} [1 - P_{jk}] \right\} . \quad (2)$$

Here we have introduced the notation

$$[dr_A] = \prod_{j=1}^{A} d^3 r_j |\phi_A(\mathbf{r}_1, \ldots, \mathbf{r}_A)|^2 \simeq \prod_{j=1}^{A} d^3 r_j \rho_A(r_j) \delta \left[\frac{1}{A} \sum_j \mathbf{r}_j \right] \quad (3)$$

to indicate the integral over the configuration of the nucleus of mass A. The nuclear density normalized to unity is $\rho_A(r)$. Appendix A lists the nuclear density functions we use in this work. The approximations we use to compute the various partial cross sections are described in Appendix B. Figure 1 shows the resulting inelastic nucleus-air cross sections for several nuclei; we use these results in all examples that follow.

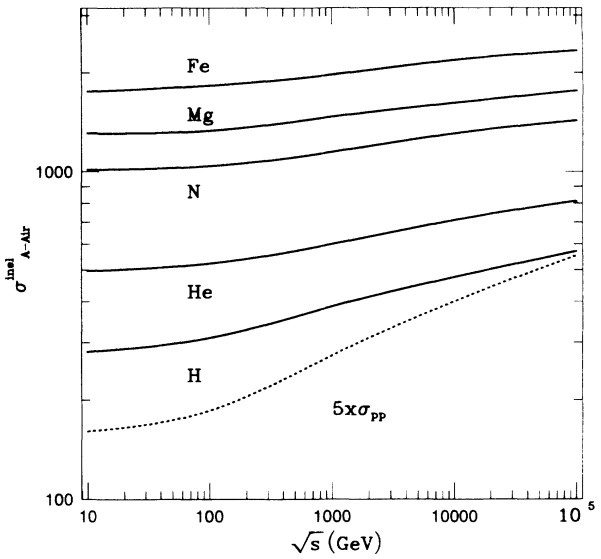

FIG. 1. Nucleus-air inelastic production cross sections as a function of $\sqrt{s}$. The pp inelastic cross section is also shown as a dotted line.

It is easy to expand this equation in terms of a "configuration" of interactions between the nucleons of the two nuclei. For example, the probability of having n participant nucleons in nucleus A is

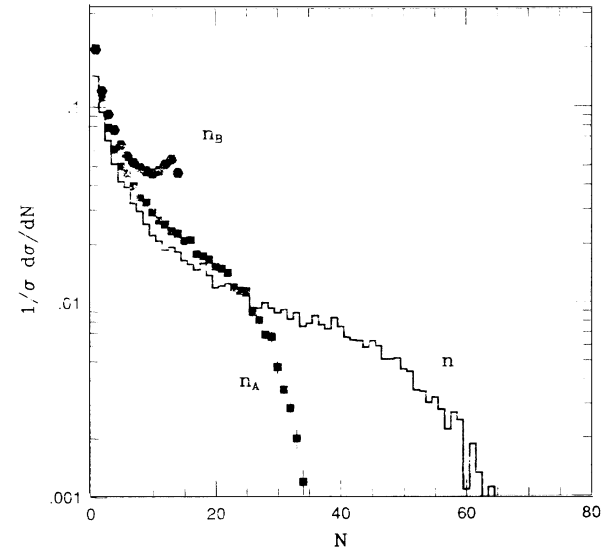

FIG. 2. Distribution of the number of interactions in iron-nitrogen collisions at $E_0 = 1 \times A$ TeV produced by the model simulation. Histogram, total number of inelastic nucleon-nucleon interactions (n); squares, number of participating nucleons in the iron projectile (n_A); hexagons, number of participating nucleons in the nitrogen target (n_B).

$$\sigma_{AB}(n_A)=\int d^2b \int [dr_A]\int [dr_B] \sum_{\{n\}} \sum_{j\in\{n\}} Q_j \prod_{l\in A-\{n\}} (1-Q_l) , \tag{4}$$

where

$$Q_j(\mathbf{b},\mathbf{t}_j,\mathbf{s}_1,\ldots,\mathbf{s}_B)=1-\prod_{k=1}^{B}[1-P(|\mathbf{b}-\mathbf{t}_j+\mathbf{s}_k|)] \tag{5}$$

is the probability that nucleon j from nucleus A interacts inelastically with at least one nucleon in nucleus B. We indicate by $\{n\}$ a set of n nucleons in nucleus A. The summation is then over all $A!/[(A-n)!n!]$ such sets. For each term the n nucleons in the set $\{n\}$ interact at least once, and the remaining $A-n$ do not interact. In the approximation that the nucleon positions in A are uncorrelated, we can use symmetry to rewrite Eq. (4) as

$$\sigma_{AB}(n_A)=\frac{A!}{(A-n)!n!}\int d^2b \int [dr_A]\int [dr_B] \prod_{j=1}^{n_A} Q_j \prod_{l=n_A+1}^{A} (1-Q_l) . \tag{6}$$

For any integer A and any set of A real numbers $(X_1,\ldots,X_A)$, we have the identities

$$\sum_{n=1}^{A} \sum_{\{n\}} \prod_{j\in\{n\}} X_j \prod_{l\in A-\{n\}} (1-X_l)=1-\prod_{k=1}^{A}(1-X_k) , \tag{7}$$

$$\sum_{n=1}^{A} n \sum_{\{n\}} \prod_{j\in\{n\}} X_j \prod_{l\in A-\{n\}} (1-X_l)=\sum_{k=1}^{A} X_k . \tag{8}$$

From these, follow the simple results

$$\sum_{n_A=1}^{A} \sigma_{AB}(n_A)=\sigma_{AB}^{\text{prod}} \tag{9}$$

and

$$\langle n_A\rangle=\frac{\sum_{n_A=1}^{A} n_A \sigma_{AB}(n_A)}{\sigma_{AB}^{\text{prod}}}=\frac{A\sigma_{pB}^{\text{prod}}}{\sigma_{AB}^{\text{prod}}} . \tag{10}$$

It is also possible to expand the production cross section as a sum over the number of nucleon-nucleon interactions. Each pair of nucleons k in nucleus A and j in nucleus B has a probability of interaction P_{jk}; the probability of having N nucleon-nucleon interactions can then be obtained by summing over all possible combinations. We indicate by $\{N\}$ a set of N pairs of one nucleon from nucleus A and one from nucleus B. Then

$$\sigma_{AB}(N)=\int d^2b \int [dr_A]\int [dr_B] \sum_{\{N\}} \prod_{j,k\in\{N\}} P_{jk} \prod_{l\in AB-\{N\}} (1-P_{lm}) . \tag{11}$$

The summation is over all $(AB)!/[(AB-N)!N!]$ possible combinations, and in each term there are exactly N nucleon-nucleon interactions. Using the identity (8) again, we can prove that

$$\langle N\rangle=\frac{AB\sigma_{pp}}{\sigma_{AB}} . \tag{12}$$

Figure 2 shows the distributions for wounded nucleons in the projectile and target in collisions of iron projectiles on nitrogen targets. Also shown is the distribution of the number of nucleon-nucleon interactions. Despite their large widths, all distributions peak at one wounded nucleon, i.e., for very peripheral collisions.

III. FRAGMENTATION OF THE RESIDUAL NUCLEUS

The ideas underlying the Glauber picture readily lend themselves to a treatment of nuclear fragmentation. Almost all fragmentation models [9] begin by dividing the projectile nucleus in any collision into participants and spectators. The collision sweeps away the participants, in the process transferring some energy to the spectators, which then fragment in accordance with some dynamics and/or statistical mechanics. To quantify this description, we need to estimate the energy deposited in the spectators and to model the subsequent decay. We are interested in the fragmentation of the projectile nucleus, which depends on the amount of energy deposited into the projectile, i.e., on the interaction properties in its frame. Thus, for testing our algorithms, we can use data taken at much lower energy, e.g., at 1 to a few hundred GeV/nucleon. (Some energy dependence might arise from a possible change in rapidity density in the fragmentation region, which contains the particles that are slow enough in the projectile frame to deposit energy in the spectators.) The majority of cosmic-ray collisions are peripheral, wounding only a few nucleons and depositing relatively little energy in the spectators. Having estimated this energy, we should therefore also be able to employ decay models developed for lower-energy beams.

We estimate the deposited energy as follows. A

wounded nucleon near the surface of the projectile nucleus will be kicked essentially perpendicular to the beam direction with kinetic energy typically less than 150 MeV. Roughly half the time it will enter what remains of the projectile (the "prefragment") and lose some of its energy in collisions with other nucleons. We estimate the amount of energy loss via the equation

$$\frac{dE}{dx} = -\alpha\rho\sigma(E)E \ , \tag{13}$$

where ρ is the nuclear density, σ is the elastic nucleon-nucleon cross section, α represents the fraction of the particle's kinetic energy lost in each collision, and dx is the element of path length in the residual nucleus. We take all of these quantities from Ref. [10].

To calculate the path lengths through the residual nucleus, we sample from a distribution corresponding to the pseudorapidity distribution of the leading nucleons in the interaction, assuming an approximate scaling. The excitation energy is obviously strongly correlated with the number of wounded nucleons. Summing over all possibilities, we find that the projectile prefragment from an iron-air collision receives on average 7 MeV of excitation energy per nucleon; about half of all collisions, however, deposited less than 3 MeV per nucleon. There is also an additional energy deposition attributable to the deformation of the prefragment surface, which we calculate following Ref. [11]. For high-energy collisions, this represents a small correction to the mechanism discussed above. Finally, we neglect any energy that may be deposited in the prefragment by secondaries. These are generally slower (in the laboratory) than the leading nucleon and enter the prefragment less often. The occasional fast pion or kaon that does enter the prefragment will, according to a calculation similar to that described above, deposit less energy than a nucleon, so that the error in neglecting it is small.

Our next assumption, also commonly made, is that the excitation energy equilibrates among all the spectators. To determine the fragmentation of the resulting prefragment, we use a model due to Friedman [3]. In this model the prefragment is a hot Fermi gas that cools by expanding adiabatically and evaporating nucleons, deuterons, and heavier clusters. The model has the advantage of describing both multifragmentation (the emission of a few intermediate-mass clusters) and the evaporation of nucleons and light clusters (usually leaving a single heavy-fragment residue) within the same physical picture. This is important because, while most of the emitted fragments are nucleons, multifragmentation is not negligible, particularly in high-energy cosmic-ray collisions, which deposit on average somewhat more energy than any accelerator can. In addition, the model predicts that if the excitation energy is very large, the prefragment disintegrates essentially completely into nucleons, a result of about $\frac{1}{4}$ of all iron-air collisions according to our energy-deposition calculation. Figure 3 compares the output of the Monte Carlo code for fragmentation of Fe on air nuclei to the data of Ref. [12] (Fe on C). No data were taken below $A_F = 34$.

Finally, we need to know the transverse momenta imparted to the various fragments. In the initial collision, when the participants are sheared away, the remaining prefragment has some net overall momentum coming from the Fermi motion of the spectators. The distribution of prefragment momenta P can be estimated in several ways. A good approximation [13] is to sample from a Gaussian $e^{-P^2/2\Delta^2}$, where $\Delta = p_F\sqrt{5n(A-n)/(A-1)}$, p_F is the Fermi momentum, and n is the number of wounded nucleons. When the nu-

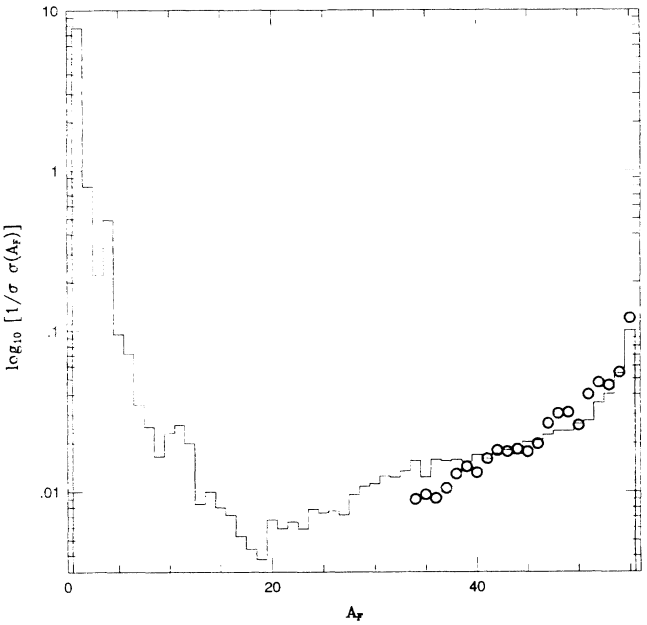

FIG. 3. Mass distribution of fragments produced in iron-nitrogen collisions at $E_0 = 1 \times A$ TeV. The histogram shows the result of the simulation; the data points are from Ref. [12] for iron collisions on carbon.

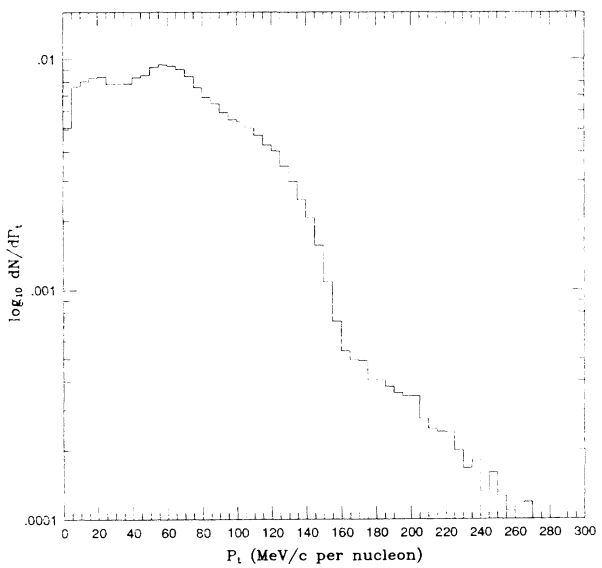

FIG. 4. Transverse momentum distribution of spectators predicted by the model for iron-nitrogen collisions at $E_0 = 1 \times A$ TeV.

cleons and clusters subsequently leave the cooling prefragment, they isotropically carry off some kinetic energy, the distribution of which is characterized by the temperature at the time of emission; this last quantity is obtained from the expanding-Fermi-gas model described above. Figure 4 shows the distribution of transverse momenta acquired by the spectator nucleons.

Together these ingredients allow us to include projectile-fragmentation properties in our shower Monte Carlo program, including the initial transverse momenta of the spectator fragments. For technical reasons we have not included the longitudinal fraction of the Fermi motion in the current version of our codes, but we will show in Sec. V that the errors due to its omission are small.

IV. DISTRIBUTION OF FIRST INTERACTIONS

Now that we have the distribution of wounded nucleons in the projectile, determined by $\sigma_{AB}(n_A)$, and a scheme for fragmenting the group of spectator nucleons, we are in a position to determine the distribution in the atmosphere of points of first interaction for all nucleons. In the semisuperposition model, this distribution specifies the subsequent development of the cascade. We consider a shower induced by a primary nucleus of mass A and define the probability of having a certain set of positions of first interaction, $\{X_1,X_2,\ldots,X_A\}$, as

$$F_A(X_1,X_2,\ldots,X_A)dX_1dX_2\cdots dX_A \ .$$

The normalization is chosen so that

$$\int \prod_{j=1}^{A} dX_j F_A(X_1,X_2,\ldots,X_A)=1 \ . \tag{14}$$

In the superposition model, we have

$$F_A(X_1,X_2,\ldots,X_A)\rightarrow \prod_{j=1}^{A}\left[\frac{e^{-X_j/\lambda_p}}{\lambda_p}\right], \tag{15}$$

where λ_p is the interaction length of a proton. In general, the function F_A will be a more complicated combination of the interaction lengths $\lambda_{A'}$ with $1\le A'\le A$ for the inelastic scattering of nucleus A' on air, of the probability $P_{A'}(n)$ of having n participating nucleons in an inelastic A-air collision, and of the branching ratios $B[(A'-n)^*\rightarrow a_1+a_2+a_f]$ for the fragmentation of the $(A'-n)$-nucleon residual nucleus into a given set of fragments (with the obvious condition $\sum_f a_f=A'-n$). As an example, consider an extreme model in which all spectator nucleons are completely freed. Then

$$F_A(X_1,\ldots,X_A)=\sum_{n=1}^{A}P_A(n)\left[\frac{\exp(-X_1/\lambda_A)}{\lambda_A}\prod_{j=2}^{n}\delta[X_j-X_1]\prod_{k=n+1}^{A}\left[\frac{\exp[-(X_k-X_1)/\lambda_p]}{\lambda_p}\theta(X_k-X_1)\right]\right] . \tag{16}$$

The most general expression is straightforward; however, it is also long and not very illuminating. An obvious feature is that the function is not factorizable, and there are correlations between the positions of the nucleons.

It is useful to define an inclusive distribution:

$$F_A^{(\mathrm{inc})}(X)=\frac{1}{A}\sum_{j=1}^{A}\left[\int\prod_{k\neq j}dX_k F_A(X_1,\ldots,X_j,\ldots,X_A)\right]_{X_j=X} . \tag{17}$$

If we consider a set of N nuclei of mass A, all of the same energy, then $F_A^{(\mathrm{inc})}(X)$ is the distribution of the positions of first interactions for all $(A\times N)$ nucleons, i.e., summed over all nuclei.

We can now state an important result.

Theorem. If the probabilities $P_A(n)$ (of having n participating nucleons when a nucleus interacts) satisfy

$$\langle n_A\rangle=\sum_{n=1}^{A}nP_A(n)=\frac{A\lambda_A}{\lambda_p} , \tag{18}$$

then independently of how the spectators fragment, we have

$$F_A^{(\mathrm{inc})}(X)=\frac{\exp[-X/\lambda_p]}{\lambda_p} . \tag{19}$$

In other words, the inclusive distribution of first interactions is identical with that of the superposition model; i.e., it is equal to the distribution one would obtain if all the nucleons arrived independently at the top of the atmosphere. From Eq. (10) we see that condition (18) does indeed hold in the semisuperposition model.

It is easy to verify this theorem in the special case of the extreme model of fragmentation described above, where it is assumed that all spectator nucleons are freed. Integrating Eq. (16) and summing over the number of wounded nucleons in the first interaction, we obtain the inclusive distribution

$$\begin{aligned}F_A^{(\mathrm{inc})}(X)&=\frac{1}{A}\sum_n P_A(n)\left[n\frac{e^{-X/\lambda_A}}{\lambda_A}+(A-n)\frac{e^{-X/\lambda_p}-e^{-X/\lambda_A}}{\lambda_p-\lambda_A}\right]\\&=\frac{\langle n\rangle}{A}\frac{e^{-X/\lambda_A}}{\lambda_A}+\left[1-\frac{\langle n\rangle}{A}\right]\frac{e^{-X/\lambda_p}-e^{-X/\lambda_A}}{\lambda_p-\lambda_A} .\end{aligned} \tag{20}$$

If we now substitute $\langle n \rangle = A\lambda_A/\lambda_p$, we obtain the result (19). Equation (20) can also be derived by observing that the first term in square brackets corresponds to the nucleons that interact and the second to the nucleons that are spectators in the first interaction. The distribution of positions of interaction for the spectators of the first interaction can be obtained by folding two exponentials:

$$\int dy \int dz \left[\frac{e^{-y/\lambda_A}}{\lambda_A} \right] \left[\frac{e^{-z/\lambda_p}}{\lambda_p} \right] \delta[y+z-X] = \frac{e^{-X/\lambda_p} - e^{-X/\lambda_A}}{\lambda_p - \lambda_A} . \tag{21}$$

This result is true in general for any spectator fragmentation scheme. A formal proof can be constructed by iterating the argument outlined above. The theorem is in some sense physically transparent; it follows from the assumptions of the Glauber picture, in which nucleons interact independently of each other and the distribution of nucleons in the nucleus is not appreciably deformed during the crossing time.

The difference between the models shows up in fluctuations from event to event, which are larger in the more realistic model. A formal treatment of fluctuations is given in Appendix C. A physical way to understand the increased fluctuations is to examine the average position of interaction of the A nucleons that compose a nucleus. Consider the average

$$\bar{X} = \frac{1}{n} \sum_{j=1}^{A} X_j . \tag{22}$$

Note that we are now averaging the A positions of first interaction from a single incident nucleus. The quantity $\bar{X}$ will have a distribution H_A that can be calculated as

$$H_A(\bar{X}) = \int \prod_{j=1}^{A} dX_j F_A(X_1, \ldots, X_A) \delta \left[\frac{1}{A} \sum_{k=1}^{A} X_k - \bar{X} \right] . \tag{23}$$

In the superposition model, this function can be computed explicitly:

$$H_A(\bar{X}) = \frac{1}{\lambda_p^A} \frac{A^A}{(A-1)!} \bar{X}^{A-1} \exp\left[-\frac{A\bar{X}}{\lambda_p} \right] , \tag{24}$$

with $\langle \bar{X} \rangle = \lambda_p$ and $\sigma_{\bar{X}} = \lambda_p/\sqrt{A}$.

In general, the function H_A will have a more complicated form. The "average of the average" $\langle \bar{X} \rangle$ will still be λ_p [because of Eq. (19)], but the fluctuations in $\bar{X}$ will be much wider. This is due to the positive correlation among the different positions of first interactions; they tend to be close together. Any quantity that is sensitive to the starting point of the shower will exhibit these properties—the same average as in the superposition model, but with broad fluctuations.

In Fig. 5 we show the distribution $H_A(\bar{X})$ for several different models for fragmentation of the residual nucleus in collisions of iron on nitrogen. In addition to the superposition model and the realistic fragmentation described in the previous section, we show two extreme models of fragmentation that bracket the realistic model. One of these extremes (also described above) assumes that the residual nucleus dissolves completely into individual nucleons and the other that the residual nucleus with $A' = A - n_A$ always remains intact as a single fragment. The latter is close to the realistic picture.

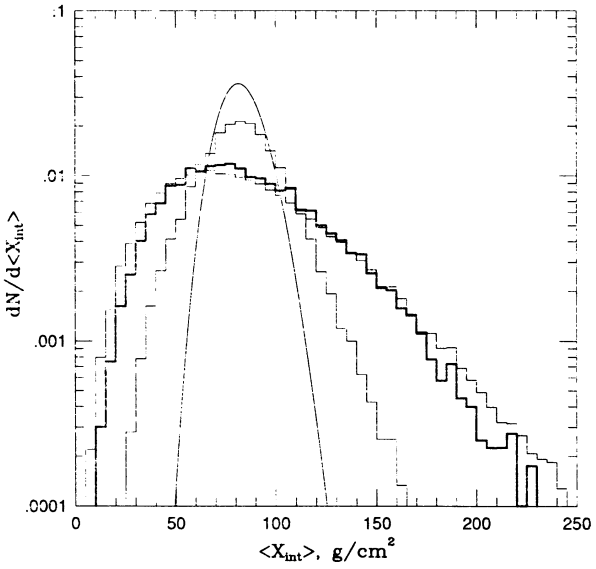

FIG. 5. Distribution of the average position of first interaction of 56 nucleons ($\bar{X}$) in atmospheric showers induced by a primary iron nucleus of energy $E_0 = 1 \times \text{TeV}$. We show the results of our fragmentation model (heavy histogram), the superposition model (curve), and the two extreme fragmentation models described in the text (light histograms).

V. APPLICATIONS

In this section we discuss some examples of the general results obtained above. We consider two directly measurable quantities that are used to determine the composition of cosmic rays. The first is the number of TeV muons generated by a primary cosmic-ray heavy nucleus. Heavy nuclei are more prolific than protons of the same total energy in production of TeV muons, and so experimental data on the multiplicity of muons in deep underground detectors is sensitive to composition. The energy range in which the relative rates of multiple muons is sensitive to composition depends on the detector depth, but includes the range from 10^{14} to 10^{16} eV, which includes the interesting "knee" region of the spectrum [14,18].

The second quantity is the position of the maximum ($X_{\max}$) in the development of a nuclear shower as measured by air-shower experiments. Showers initiated by heavier nuclei dissipate their energy faster than proton showers, thus having shallower $X_{\max}$. The aim of the

work presented in this section is to determine the size of the corrections to the superposition model from a realistic treatment of the positions of first interactions. The application of the results to any experiment will necessarily involve a detailed account of fluctuations due to detector resolution. In the Monte Carlo calculations presented in this section, we have used a simple model of p-air and π-air interactions, originally developed by Hillas [17], which exhibits Feynman scaling. Realistic interpretation of data will require use of a more realistic hadronic interaction model, as well as detailed treatment of detector-dependent selection effects, but that is not our purpose here.

A. High-energy muons

As an example, we consider the number of high-energy muons $E_\mu \geq 1$ TeV produced by a vertical iron nucleus ($A=56$) of total energy $E_{\rm tot}=A\times 100$ TeV. In Fig. 6 we show the muon multiplicity distribution $P(N_\mu)$ calculated in superposition and semisuperposition. The curves superimposed on the Monte Carlo points show negative binomial distributions with the same averages and dispersions as the points. They are a good fit to the Monte Carlo results. As expected, both distributions have the same average $\langle N_\mu \rangle = 30.0$, but different widths. The superposition model generates a nearly Poissonian distribution with $\sigma(N_\mu)=5.9$; in the more realistic case, $\sigma(N_\mu)=7.5$. The extreme fragmentation models (not shown in the figure) give $\sigma(N_\mu)=6.8$ and 7.9. Considering the steepness of the cosmic-ray spectrum, these seemingly small differences could have an impact on the interpretation of data.

The transverse momentum gained by the spectator nucleons and fragments in the nuclear fragmentation do not affect noticeably the lateral spread of the muons in the bundle. Formally, one would expect the contribution in the separation to be of the order

$$r_F \sim \frac{p_F}{E_0}\frac{200}{E_0(\text{TeV})\cos\theta}\ \text{cm}\ .$$

Added in quadrature to the separation due to the transverse momentum gained in the interaction, this is not an observable effect. The average displacement of TeV muons produced by iron nuclei of energy 10 TeV/nucleon is ~ 2 cm, as compared to several meters for typical separations of multiple muons deep underground. This effect, however, may not be negligible for different types of cosmic-ray experiments. In particular, the average additional displacement by 2 cm might be significant for the interpretation of the results on γ and hadron families in mountain emulsion chambers, where it would be comparable to the lateral spread of the family due to transverse momentum gained in the interaction.

An effect that *is* potentially important is the correlation between multiplicity and separation. Two circumstances give rise to events with large numbers of muons: A large amount of energy goes into charged rather than neutral pions and/or the shower starts high in the atmosphere where the relative probability of meson decay (rather than interaction) is greater [16]. These two factors depend on the underlying hadronic interaction model. The correlation between height of origin and multiplicity gives rise to a correlation between multiplicities which depends on the nuclear fragmentation model. Since the $\langle X_{\rm int} \rangle$ distribution is wider for the semisuperposition model, the range of variation in the lateral spread is correspondingly bigger. The size of this effect can be estimated from distribution of $\bar{X}$ shown in Fig. 5. In the example shown, for the superposition model, 80% of the events have $\bar{X}$ between 68 and 95 g/cm^2, whereas in the realistic fragmentation model the corresponding depths are 43 and 140 g/cm^2. The corresponding effective heights of origin are 16.3 ± 1 and $\sim 16.3^{+4}_{-3.5}$ km. Thus

$$r_{\rm eff} \sim \langle r \rangle (1\pm 0.06)\ \text{superposition}$$

and

$$r_{\rm eff} \sim \langle r \rangle (1^{+0.25}_{-0.22})\ \text{realistic fragmentation}\ .$$

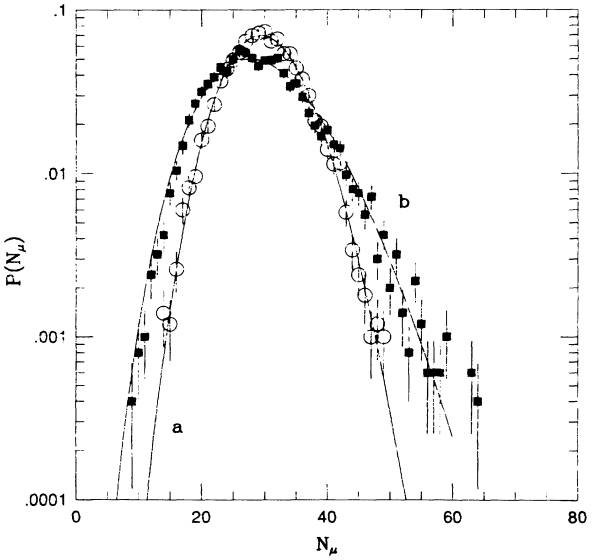

FIG. 6. Distribution of the number of muons with $E_\mu \geq 1$ TeV produced by a vertical (zenith angle $\theta=0°$) iron nucleus of energy $E_0=100\times A$ TeV simulated in the superposition (circles) and the semisuperposition (solid squares) models. The curves show negative-binomial distributions with the averages and dispersions fit to the simulated data.

B. Size development

Here we consider fluctuations in shower size (number of electrons) for nuclear showers as a function of atmospheric depth. We have simulated iron showers and calculated the maximum depth $X_{\rm max}$ and shower size $S(X)$. In the superposition model, the position of the maximum and the shower size are almost fully determined by the energy of the primary nucleus. The increased fluctuations of $\bar{X}$ induce corresponding fluctuations in $X_{\rm max}$. Figure 7 shows the distributions of $X_{\rm max}$ for iron showers of total energy 10^{18} eV developing at a zenith angle of 45°, calculated in the superposition and semisuperposi-

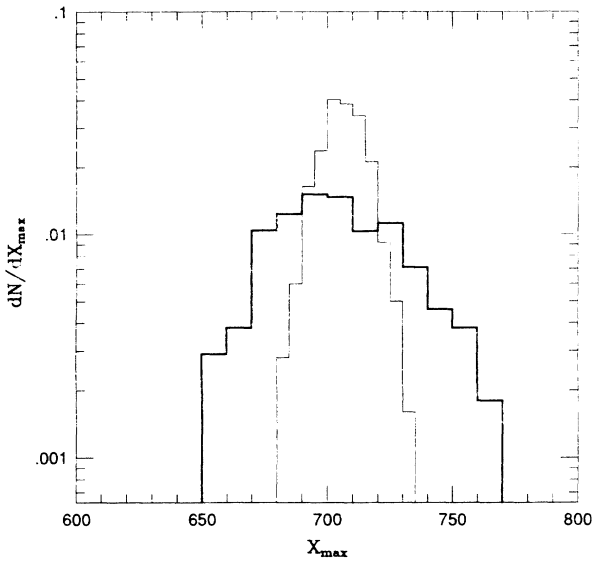

FIG. 7. Distributions of $X_{\max}$, the position of the maximum size, for showers induced by a primary iron nucleus of total energy $E_{\rm tot}=10^{18}$ eV and zenith angle $\theta=45°$, calculated in the semisuperposition (heavy histogram) and superposition (light histogram) models.

tion models. The two yield the same average $\langle X_{\max}\rangle=700$ g cm^{-2}, but exhibit quite different widths. In the superposition model, $\sigma(X_{\max})=9$ g cm^{-2}, whereas in the more realistic semisuperposition model the width is about 3 times larger, $\sigma(X_{\max})=25$ g cm^{-2}. The extreme fragmentation models give dispersions correspondingly of $\sigma(X_{\max})=21$ and 29 g cm^{-2}. For comparison, a proton shower of the same energy has $\sigma(X_{\max})=59$ g cm^{-2}. Inclusion of realistic fluctuations for nuclear primaries gives a significant improvement in matching the $X_{\max}$ distribution observed by the Fly's Eye [18].

VI. LIMITATIONS OF THE SEMISUPERPOSITION MODEL

In the semisuperposition model, each participant nucleon in the projectile is treated as if it interacted independently with an air nucleus (though often at the same macroscopic point as other nucleons). The real physics of the interaction is quite different. In the semisuperposition model, interesting correlations, easily understandable on geometrical grounds, are left out. For example, if $n_A=1$, the nucleus-nucleus collision is very likely peripheral, and the interaction will look very much like a p-p interaction. In this case the single wounded nucleon in the projectile will probably not interact more than once inside the target. At the other extreme, a large n_A signals a central collision in which each participating nucleon in the projectile has a high probability of interacting several times in the target and vice versa. Such a collision will likely have a softer distribution of produced particles than a sum of nucleon-air interactions.

In addition to omitting these correlations, the semisuperposition model also systematically distorts the inclusive rapidity distribution averaged over all types of events. This occurs for the following reason: In a hadron-air collision, each wounded nucleon in the target interacts exactly once. In a nucleus-nucleus collision, the wounded nucleons in the target can interact more than once. Thus, if we correctly specify the average number of participating nucleons in the projectile and treat each one as a nucleon-air interaction, we are bound to have too many participating nucleons in the target. The semisuperposition model, therefore, overestimates the production of particles in the backward (target) hemisphere. Figure 8 shows the pseudorapidity distribution for an iron-nitrogen interaction calculated in two ways: (a) in the semisuperposition model and (b) with a correct treatment of the participating nucleons in the target as well as the projectile. In (a) the distribution is

$$\left[\frac{dn}{d\eta}\right]_{AB}\simeq\langle n_A\rangle_{AB}\left[\frac{dn}{d\eta}\right]_{pB}, \tag{25}$$

which gives an excess on the target side.

On the projectile side, away from the central region, the two distributions are essentially the same. It is this feature that justifies the use of the semisuperposition model to estimate some features of cascades, because the development of showers is sensitive primarily to the forward region. In the remainder of this section, we discuss how the features illustrated in Fig. 8 arise in a class of "multistring" models (see also Fig. 9).

Multistring models [5,7] are those in which hadronic interactions are modeled as the formation and subsequent fragmentation of a set of color strings. A proton-nucleus interaction with n_B participating nucleons in the target is modeled in leading order as the formation and fragmentation of $2n_B$ color strings. The projectile proton "splits"

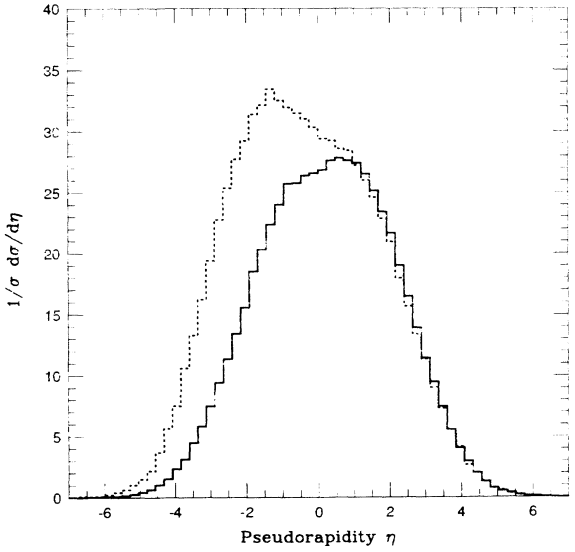

FIG. 8. Pseudorapidity distribution for charged particles in an iron-nitrogen (solid histogram) collision at $\sqrt{s}=43.3$ GeV/nucleon, compared with the inclusive distribution for proton-nitrogen collisions rescaled by a factor $\langle n_{\rm Fe}\rangle_{\rm Fe\text{-}N}$ (dotted histogram).

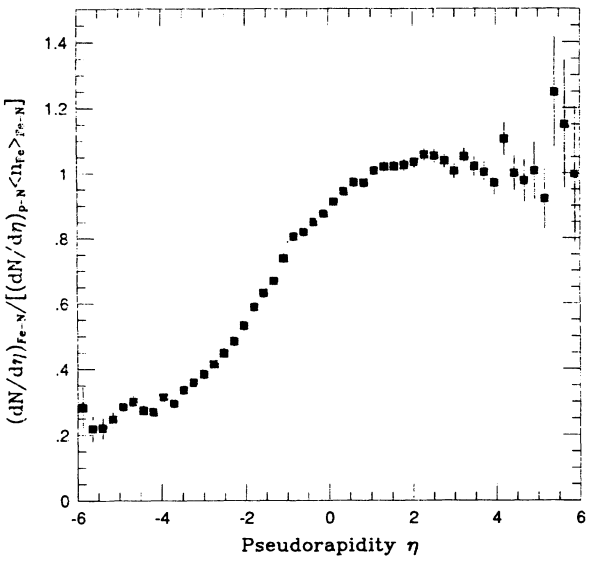

FIG. 9. Ratio $R(\eta)$ of iron to proton pseudorapidity distributions for charged particles in collisions with nitrogen, with the inclusive distribution in proton-nitrogen collisions rescaled by a factor $\langle n_{\mathrm{Fe}} \rangle_{\mathrm{Fe\text{-}N}}$.

into $2n_B$ components: two valence components (a diquark and a quark) and (n_B-1) quark-antiquark pairs, with fractional energy distribution $\rho(x_1,\ldots,x_{2n_B})$. Each wounded target nucleon is decomposed into two valence components. Pairs of partons of opposite color (one from the projectile and one from the target) are then paired together to form color strings that fragment into physical particles.

In a nucleus-nucleus interaction, a participating nucleon that interacts with n_B target nucleons will again split into $2n_B$ components with the same fractional energy distribution. Partons of opposite color in the projectile and in the target are again paired to form a total of $2N_{\mathrm{int}}$ strings (where N_{int} is the total number of nucleon-nucleon inelastic interactions in the collision). In this case, however, quark-antiquark pairs from the target sea may also be involved.

At high c.m. energy, the "partonic structure" of an interaction becomes more complex, and more color strings are formed. This additional structure can be interpreted as arising from parton-parton semihard scatterings (minijets) [19] or as an expansion in the number of cut Pomerons [20,5]. We will not discuss these important complications here [8]. The arguments we are developing remain valid (neglecting small kinematical effects) even including these higher-order terms.

We now state some well known properties of the fragmentation of color strings. Let us consider a color string produced by a parton at the projectile side of fractional energy x_1 and flavor q_1 and a target parton of fractional energy x_2 and flavor q_2. The string will have a mass $M=\sqrt{sx_1x_2}$ and, in the c.m. frame of the nucleon-nucleon scattering, will move with velocity $\beta=(x_1-x_2)/(x_1+x_2)$. Let $f(y,M,q_1,q_2)$ be the rapidity distribution of the particles produced in the fragmentation of this string. The kinematical limits for the production of a particle of mass m are

$$y_{\max}=\ln\left[\frac{\sqrt{s}}{m}x_1\right],\quad y_{\min}=-\ln\left[\frac{\sqrt{s}}{m}x_2\right], \tag{26}$$

which depend only on the fractional energy of a single parton. The entire rapidity range is $(y_{\max}-y_{\min})=2\ln(M/m)$. For M not too small, two properties follow from the dynamics of string fragmentation [7].

(i) The shape of the rapidity distribution in the limit $y\to y_{\max}$ depends only on the flavor q_1 and is independent of the mass M and the other flavor q_2. (Symmetrically, the rapidity spectrum for $y\to y_{\min}$ depends only on the flavor q_2.)

(ii) In the central region, there is a rapidity plateau with properties that are independent of q_1, q_2, and the mass of the string.

Item 1 assures that the semisuperposition model gives the correct rapidity distribution in the forward region. It follows from the basic structure of the multiple-scattering framework of Sec. II that the distribution of the number collisions suffered by a single wounded nucleon in a projectile nucleus is independent of the mass of the projectile. The distribution is the same as the distribution of wounded-nucleon number in the target for projectile protons. Nucleus-nucleus and proton-nucleus collisions are distinguished by the fact that the "projectile partons" are paired together with "target partons" that have different flavor and energy distributions for the two cases. The inclusive spectrum is the sum of the spectra produced by the different strings. Because the spectra and flavor distributions of the particles produced in the fragmentation of the "forward part" of the string are independent of the mass of the string and of the flavor attached to the other end, the inclusive distribution will be equal over a large part of the forward hemisphere to what is obtained by superimposing nucleon-nucleus interactions.

We can also clarify, from similar considerations, the reason that the semisuperposition spectrum $\langle n_A \rangle_{BA}(dn/dy)_{pB}$ is significantly larger than the nucleus-nucleus spectrum in the backward hemisphere. The total number of color strings is on average the same in the two situations, but in the case of nucleus-nucleus interactions the number of participating nucleons in the target is lower, and a larger number of strings will be short (i.e., coupled to $q\bar{q}$ pairs from the target sea). The particle-particle rapidity correlation length in string fragmentation is of the order of a unit in rapidity, and therefore the two spectra (the semisuperposition and the nucleus-nucleus) will differ also in the forward hemisphere for one or two units of rapidity.

To demonstrate the validity of our approach, we simulated nuclear collisions using a full Monte Carlo program, incorporating the physics described above, in nucleus-nucleus collisions at 200 GeV/nucleon and compared the output with experiment [21]. For ^{16}O on a target mixture of 20% He and 80% Ne, the experiment yielded distributions with averages of 47.8 charged particles and 17.3 negatively charged particles and standard deviations of 32.8 and 13.8, respectively, while our Monte

Carlo program generated averages of 39.1 and 17.9 for charged and negatively charged multiplicities, with standard deviations of 31.3 and 14.5. For the same beam on Cu ($A=63.5$), the experimental averages for charged and negative multiplicities were 81.5 and 35.7, with standard deviations 64.0 and 27.9. Our Monte Carlo calculation with an iron target ($A=56$) yielded 76.4 and 35.1 as averages, with standard deviations of 73.7 and 34.2, respectively. The Monte Carlo calculation apparently reproduces the multiplicity of negatively charged particles quite well. The differences in the total charged multiplicity are mostly due to the omission from our calculation of spectator protons and light fragment nuclei. The widths of the calculated multiplicity distributions are also very similar to the experimental ones, although our Monte Carlo code seems to generate slightly wider distributions. It is not our aim to make exact comparisons to data at this stage of model development. The good agreement of both the average multiplicities and the widths of the distributions indicates that the basic quantities we use in the semisuperposition model are sensible.

VII. CONCLUSIONS

The main point we wish to make in this paper is that a realistic treatment of incident cosmic-ray nuclei leads to showers with significantly larger fluctuations than are expected in the superposition model. This fact will undoubtedly affect the interpretation of air-shower data. A semisuperposition model is a convenient way to represent the effects of nuclear fragmentation within existing cascade codes. Generalization to a more detailed treatment of target nucleons as well as projectile constituents is certainly possible.

An earlier attempt to include effects of fluctuations [22] was based on a library of fragmentation of cosmic-ray nuclei in emulsion. The analysis was complicated by the need to select events on "airlike" targets and the indirect procedure by which the number of projectile wounded nucleons was inferred. Although that model gave a more realistic representation of fluctuations in nuclear showers than the simple superposition model, the conclusions of that study are quantitatively different from those presented here because the number of wounded nucleons in nuclear collisions extracted from the experimental data did not satisfy the basic equation (12). As a consequence, the *average* values of shower properties calculated in Ref. [22] differ from those calculated in the superposition model and that work is superseded by the present model.

Effects of nuclear primaries may also arise in the context of uncorrelated fluxes of secondary cosmic rays—for example, in recent calculations of atmospheric neutrino fluxes [23]. However, because calculating uncorrelated fluxes involves an average over many incident primary nuclei, the arguments of Secs. II and IV ensure that semisuperposition and simple superposition will give the same value for these fluxes.

In a subsequent paper, we will explore further the effect of including the nucleus-nucleus correlations discussed in Sec. VI that are omitted in the semisuperposition model.

ACKNOWLEDGMENTS

We are grateful to W. A. Friedman for providing us with numerical results from his nuclear fragmentation codes; we have used them in our cascade Monte Carlo program. This work was supported in part by the National Science Foundation under Grants Nos. PHY-9108011 and PHY-8915189.

APPENDIX A: NUCLEAR DENSITIES

For nuclear density profiles, we have used simple shell-model wave functions for nuclei with $6 \le A \le 18$ and a Woods-Saxon shape for heavier nuclei [24]. In the simple shell model for values of A given above, the nuclear density has the form

$$\rho(r)=\frac{4}{\pi^{3/2}r_0^3}\left[1+\frac{1}{6}(A-4)\frac{r^2}{r_0^2}\right]e^{-r^2/r_0^2}, \tag{A1}$$

where the normalization is chosen so that

$$\int d^3r\,\rho(r)=1\ . \tag{A2}$$

The average radius is

$$\langle r^2\rangle=\left[\frac{5}{2}-\frac{4}{A}\right]r_0^2\ . \tag{A3}$$

In the Woods-Saxon model, the nuclear density has form

$$\rho(r)=\frac{c_0}{1+\exp[(r-r_0)/a_0]}\ , \tag{A4}$$

with a normalization constant

$$c_0=\frac{3}{4\pi r_0^3}\frac{1}{1+(a_0\pi/r_0)^2}\ . \tag{A5}$$

For the two parameters r_0 and a_0, we have used the values listed in Refs. [24,25].

In He, following Ref. [24], we have used the "parabolic Fermi distribution"

$$\rho_{\mathrm{He}}(r)=C\frac{1}{1+\exp[(r-r_0)/a_0]}\left[1+w\frac{r^2}{r_0^2}\right], \tag{A6}$$

with $r_0=0.964$ fm, $a_0=0.322$ fm, and $w=0.517$.

APPENDIX B: APPROXIMATIONS AND DEFINITIONS

The nucleon-nucleon profile function $\Gamma(b)$ is the Fourier transform of the elastic-scattering amplitude:

$$\Gamma(b)=\frac{1}{2\pi ik}\int d^2q\,e^{-i\mathbf{q}\cdot\mathbf{b}}f(q)\ . \tag{B1}$$

From the relations

$$\sigma_{\mathrm{tot}}=\frac{4\pi}{k}\mathrm{Im}f(0)\ , \tag{B2}$$

$$\sigma_{\mathrm{el}}=\int|f(q)|^2d\Omega_{k'}\ , \tag{B3}$$

and

$$\sigma_{\text{inel}}=\sigma_{\text{tot}}-\sigma_{\text{el}} , \tag{B4}$$

where $\mathbf{q}=\mathbf{k}-\mathbf{k}'$, one obtains the following expressions for the cross sections in terms of the profile functions:

$$\sigma_{\text{tot}}=\int d^2b\, 2\,\text{Re}[\Gamma(b)] , \tag{B5}$$

$$\sigma_{\text{el}}=\int d^2b\,|\Gamma(b)|^2 , \tag{B6}$$

and

$$\sigma_{\text{inel}}=\int d^2b\,[1-|1-\Gamma(b)|^2] . \tag{B7}$$

The last equation makes clear the interpretation of

$$P(b)=1-|1-\Gamma(b)|^2 \tag{B8}$$

as the probability that nucleons at impact parameter b undergo an inelastic interaction. Analogous interpretations, with additional variables denoting relative nucleon position in the nucleus, hold at the nuclear level.

The partial cross sections of Sec. II are evaluated by Monte Carlo integration. In the process the full structure of the event is generated: the number of inelastically wounded nucleons in the projectile and target, the number of inelastic interactions, and the number of elastically scattered nucleons in the projectile and target. The calculations are done for a variety of incident nuclei, including $A=1$.

For these calculations two approximations to the formulas of Sec. II are made. We illustrate them here for the case of projectile mass $A=1$ and target mass B. The generalization to incident nuclei is straightforward.

Approximation 1. The equations are much simplified if we neglect the delta function in Eq. (3). This is a conventional approximation of limited validity. It is valid if the collective momentum variable conjugate to the center-of-mass coordinate can be replaced by zero in relevant expressions. Roughly, if one is calculating the expectation value of an n-body operator, then conjugate momenta $K>1/(R\sqrt{B-n})$ will be suppressed, where R is the nuclear radius. When correlations involving higher-body operators ($n>1$) are treated carefully, this approximation needs to be reconsidered.

Here we make the approximation of neglecting the δ function and introduce the notation

$$\bar{P}_B(b)=\int d^3r\,\rho_B(r)P(\mathbf{b}-\mathbf{r}) . \tag{B9}$$

Then

$$\sigma_{\text{prod}}=\int d^2b\,[1-(1-\bar{P}_B)^B] \tag{B10}$$

and

$$\sigma_n=\int d^2b \begin{pmatrix} B \\ n \end{pmatrix} \bar{P}_B^n(1-\bar{P}_B)^{B-n} . \tag{B11}$$

The average number of wounded nucleons can be calculated as

$$\langle n\rangle=\frac{1}{\sigma_{\text{prod}}}\sum_n n\sigma_n=\frac{B\sigma_{hp}^{\text{inel}}}{\sigma_{hB}^{\text{prod}}} , \tag{B12}$$

where we have used the identity

$$\sum_{k=1}^{N} k \begin{pmatrix} N \\ k \end{pmatrix} x^k(1-x)^{N-k}=Nx \tag{B13}$$

and

$$\int d^2b\,\bar{P}_B(b)=\int d^2b\,P(b)=\sigma_{hp}^{\text{inel}} . \tag{B14}$$

Approximation 2. We also use the point nucleon approximation, in which $P(b)=\delta^2[b]\sigma_{hp}^{\text{inel}}$. In this case,

$$\bar{P}_B(b)=T_B(b)\sigma_{hp}^{\text{inel}} , \tag{B15}$$

where

$$T_B(b)=\int_{-\infty}^{+\infty} dz\,\rho_B(z) . \tag{B16}$$

Substituting in (B10) and (B11), we obtain some often-used approximations. The expressions (B15) and (B16) are used to compute $\sigma_{AB}^{\text{prod}}$ and related quantities. Corresponding expressions with $\sigma_{hp}^{\text{inel}}\to\sigma_{hp}^{\text{el}}$ are used in appropriate combinations to compute quasielastic quantities.

The values of key quantities at several energies of interest are listed in Table I.

TABLE I. (a) Cross sections at $\sqrt{s}=10$ GeV ($\sigma_{pp}^{\text{inel}}=32.1$ mbarn, $\sigma_{pp}^{\text{el}}=7.4$ mbarn). (b) Cross sections at $\sqrt{s}=10^3$ GeV ($\sigma_{pp}^{\text{inel}}=54.5$ mbarn, $\sigma_{pp}^{\text{el}}=19.98$ mbarn). (c) Cross sections at $\sqrt{s}=10^5$ GeV ($\sigma_{pp}^{\text{inel}}=110.9$ mbarn, $\sigma_{pp}^{\text{el}}=90.9$ mbarn).

	$A=4$	$A=16$	$A=28$	$A=56$
		(a)		
σ_{prod}	496.0	970.0	1103.0	1471.0
σ_{qe}	37.0	51.0	44.0	77.0
$\langle n_P\rangle$	2.14	4.37	6.40	10.32
$\langle n_T\rangle$	2.64	4.42	4.74	5.38
$\langle n_{\text{int}}\rangle$	3.68	7.73	11.06	17.79
$\langle n_P^{\text{el}}\rangle$	0.20	0.49	0.79	1.31
$\langle n_T^{\text{el}}\rangle$	0.37	0.47	0.43	0.42
		(b)		
σ_{prod}	595.0	1179.0	1239.0	1674.0
σ_{qe}	78.0	98.0	109.0	114.0
$\langle n_P\rangle$	2.33	5.10	7.76	13.02
$\langle n_T\rangle$	3.25	5.14	5.55	6.94
$\langle n_{\text{int}}\rangle$	5.12	11.21	17.15	28.72
$\langle n_P^{\text{el}}\rangle$	0.27	0.75	1.31	2.21
$\langle n_T^{\text{el}}\rangle$	0.70	0.76	0.76	0.70
		(c)		
σ_{prod}	826.0	1448.0	1527.0	1999.0
σ_{qe}	241.0	311.0	351.0	361.0
$\langle n_P\rangle$	2.57	6.06	9.15	14.84
$\langle n_T\rangle$	4.01	5.62	6.12	7.17
$\langle n_{\text{int}}\rangle$	7.52	18.84	28.46	44.17
$\langle n_P^{\text{el}}\rangle$	0.61	2.01	3.30	5.46
$\langle n_T^{\text{el}}\rangle$	1.93	1.96	1.77	1.76

APPENDIX C: FLUCTUATIONS

The difference between a true nucleus shower and the superposition-model shower arises because the positions of first interaction for the A nucleons of a nucleus are strongly correlated with each other. These correlations are ignored in the superposition model. We can define a two-point distribution $F_A^{(2)}(Y_1,Y_2)$ (the probability of having two different interactions, one at Y_1 and one at Y_2) and a correlation function $C_A(Y_1,Y_2)$ by

$$F_A^{(2)}(Y_1,Y_2)=\frac{2}{A(A-1)}\sum_{j<k}\left[\int\prod_{l\neq j,k}dX_l F_A(X_1,X_2,\ldots,X_A)\right]_{Y_1=X_j,Y_2=X_k} \tag{C1}$$

$$=\frac{e^{-Y_1/\lambda_p}}{\lambda_p}\frac{e^{-Y_2/\lambda_p}}{\lambda_p}[1+C_A(Y_1,Y_2)]\ . \tag{C2}$$

The function $C_A(X_1,X_2)$ vanishes in the superposition model, but in general is positive. This is clearly due to the fact that in a nuclear collision several nucleons interact at the same point.

Having defined an appropriate correlation function, we now consider an additive physical observable Q (for example, the number of muons or electrons at a certain depth produced by the shower, but *not* the depth of the maximum, which depends logarithmically on A). We define $G_p(Q)$ to be the probability that a proton shower will result in the value Q for the observable (in this discussion we are considering the zenith angle and energy per nucleon, E_0, fixed).

In the superposition model, the probability $G_A(Q)$ that the shower of a nucleus of mass A (and same energy per nucleon) will result in a value Q for the same observable is simply the convolution of A proton distributions:

$$G_A(Q)=\int\prod_{k=1}^{A}dQ_k G_p(Q_k)\delta[(Q_1+\cdots+Q_A)-Q]\ . \tag{C3}$$

From this assumption follow the expected results:

$$\langle Q\rangle_A=A\langle Q\rangle_p\ , \tag{C4}$$

$$(\sigma_Q^2)_A\equiv\langle Q^2\rangle_A-\langle Q\rangle_A^2=A(\sigma_Q^2)_p\ . \tag{C5}$$

[Note that, as a consequence of Eq. (B14), the *relative* fluctuations in nuclear showers are, of course, smaller than those in proton showers.]

As we have noted, if we use the semisuperposition model and theorem (19), then Eq. (C4) is still valid; that is, the average value of a given quantity predicted by the simple superposition model is still correct. The fluctuations, however, are larger than what is predicted by (C5).

To prove this statement, we start by defining the function $G_p'(Q,X)dX$ as the distribution of the quantity Q for proton showers that have the first interaction between X and $X+dX$. This quantity obviously satisfies the condition

$$\int_0^\infty dX\frac{e^{-X/\lambda_p}}{\lambda_p}G_p'(Q,X)=G_p(Q)\ . \tag{C6}$$

Then the distribution of the quantity Q in the showers of nucleus A in the semisuperposition model can be written as

$$G_A(Q)=\int\prod_{j=1}^{A}dX_j F_A(X_1,\ldots,X_A)\int\prod_{k=1}^{A}dQ_k G_p'(Q_k,X_k)\delta[(Q_1+\cdots+Q_A)-Q]\ . \tag{C7}$$

Then

$$\langle Q\rangle_A=\int dQ\,QG_A(Q)=A\int dX\,F_A^{(\mathrm{inc})}(X)G_p'(Q,X)Q \tag{C8}$$

$$=A\langle Q\rangle_p\ . \tag{C9}$$

Equation (C8) is true in general. To obtain (C9), we have used the result (19).

Similarly, with the help of Eq. (19), we can show

$$\langle Q^2\rangle_A=\int dQ\,Q^2G_A(Q)=A\langle Q^2\rangle_p+A(A-1)\langle Q\rangle_p^2+\langle C_Q\rangle\ , \tag{C10}$$

so that

$$(\sigma_Q^2)_A=A(\sigma_Q^2)_p+\langle C_Q\rangle\ , \tag{C11}$$

where

$$\langle C_Q \rangle = \int dX_1 \int dX_2 \frac{e^{-X_1/\lambda_p}}{\lambda_p} \frac{e^{-X_2/\lambda_p}}{\lambda_p} C_A(X_1,X_2) \langle Q_p(X_1) \rangle \langle Q_p(X_2) \rangle \ . \tag{C12}$$

Thus the width of the distribution for the quantity Q depends on the correlation among the positions of first interactions of the nucleons that compose the nucleus. The stronger this correlation is, the wider the fluctuations.

[1] R. Glauber, in *Lectures in Theoretical Physics*, edited by A. O. Barut and W. E. Brittin (Interscience, New York, 1959); R. J. Glauber and G. Matthiae, Nucl. Phys. **B21**, 135 (1970).

[2] A. Bialas, M. Bleszynski, and W. Czyz, Nucl. Phys. **B111**, 461 (1976).

[3] See, e.g., W. A. Friedman, Phys. Rev. C **42**, 667 (1990); W. A. Freidman and W. G. Lynch, *ibid.* **28**, 16 (1983).

[4] Paolo Lipari, R. S. Fletcher, T. K. Gaisser, and Todor Stanev, in *Proceedings of the 22nd International Cosmic Ray Conference*, Dublin, Ireland, 1991, edited by M. Cawley *et al.* (Dublin Institute for Advanced Studies, Dublin, 1992), Vol. 4, p. 197; and (in preparation).

[5] A. Capella and J. Tran Thanh Van, Z. Phys. C **10**, 249 (1981).

[6] B. Andersson, G. Gustafson, and B. Nilsson-Almquist, Nucl. Phys. **B281**, 289 (1987); B. Nilsson-Almquist and E. Stenlund, Comput. Phys. Commun. **43**, 387 (1989).

[7] T. Sjöstrand and M. van Zijl, Phys. Rev. D **36**, 2019 (1987); H. Bengtsson and T. Sjöstrand, Comput. Phys. Commun. **46**, 43 (1987).

[8] X.-N. Wang and M. Gyulassy, Phys. Rev. D **44**, 3501 (1991).

[9] For a review, see J. Hufner, Phys. Rep. **125**, 129 (1985).

[10] L. F. Olveira, R. Donnagelo, and J. O. Rasmussen, Phys. Rev. C **19**, 826 (1979).

[11] J. Hufner, K. Schafer, and B. Schurmann, Phys. Rev. C **12**, 1888 (1975).

[12] W. R. Webber, J. C. Kish, and D. A. Schrier, Phys. Rev. C **41**, 547 (1990).

[13] A. Abul-Madg and J. Hufner, Z. Phys. A **277**, 379 (1976).

[14] G. Auriemma, S. Bussino, T. K. Gaisser, and Todor Stanev, in *Proceedings of the 22nd International Cosmic Ray Conference* [4], Vol. 2, p. 101.

[15] MACRO Collaboration, S. Ahlen *et al.*, Phys. Rev. D **46**, 895 (1992).

[16] H. Bilokon *et al.*, in *Proceedings of the 21st International Cosmic Ray Conference*, Adelaide, Australia, 1990, edited by R. J. Protheroe (Graphic Services, Northfield, South Australia, 1990), Vol. 9, p. 114.

[17] H. M. Hillas, in *Proceedings of the 17th International Cosmic Ray Conference*, Paris, France, 1981 (CEN, Saclay, 1981), Vol. 8, p. 183.

[18] T. K. Gaisser *et al.*, in *Proceedings of the 22nd International Cosmic Ray Conference* [4], Vol. 4, p. 413; and unpublished.

[19] T. K. Gaisser and Todor Stanev, Phys. Lett. B **219**, 375 (1989).

[20] B. Z. Kopeliovich, N. N. Nikolaev, and I. K. Potashnikova, Phys. Rev. D **39**, 769 (1989).

[21] NA35 Collaboration, A. Bamberger *et al.*, Phys. Lett. B **205**, 583 (1988).

[22] T. K. Gaisser, T. Stanev, P. Freier, and C. J. Waddington, Phys. Rev. D **25**, 2341 (1982).

[23] G. Barr, T. K. Gaisser, and Todor Stanev, Phys. Rev. D **39**, 3532 (1989); E. V. Bugaev and V. A. Naumov, Phys. Lett. B **232**, 391 (1989); H. Lee and Y. S. Koh, Nuovo Cimento B **105**, 883 (1990); M. Honda, K. Kasahara, K. Hidaka, and S. Midorikawa, Phys. Lett. B **248**, 193 (1990); M. Kawasaki and S. Mizuta, Phys. Rev. D **43**, 2900 (1991).

[24] R. C. Barrett and D. F. Jackson, *Nuclear Sizes and Structure* (Oxford University Press, New York, 1977).

[25] J. Eisenberg and W. Greiner, *Excitation Mechanisms of the Nucleus, Nuclear Theory,* Vol. 2 (North-Holland, Amsterdam, 1970).